Structural and optical properties of Ag:TiO_2 nanocomposite films prepared by magnetron sputtering

R. C. ADOCHITE , M. TORRELL[*], L. CUNHA, E. ALVES[a], N. P. BARRADAS[a], A. CAVALEIRO[b], J. P. RIVIERE[c], D. EYIDI[c], F. VAZ

Centro de Física, Universidade do Minho, Campus de Azurém, 4800-058 Guimarães, Portugal
[a]Instituto Tecnológico e Nuclear, Dept. Física, Apartado 21, E.N. 10, 2686-953 Sacavém, Portugal
[b]SEC-CEMUC – Universidade de Coimbra, Dept. Eng. Mecânica, Polo II, 3030-788 Coimbra, Portugal
[c]Institut Pprime, UPR 3346-CNRS-Université de Poitiers-ENSMA, SP2MI, téleport 2, Bd M. et Pierre Curie, BP 30179, 86962 Futuroscope-Chasseneuil, France

Three sets of nanocomposite films consisting of different atomic concentrations of Ag dispersed in a TiO_2 dielectric matrix were deposited by DC reactive magnetron sputtering, and subjected to several thermal annealing experiments in vacuum, for temperatures ranging from 200 to 600 ºC. The main goal of the present study is to analyse the optical properties of the as-deposited and annealed films in order to clarify the role of Ag inclusions in the TiO_2 dielectric matrix. The influence of the thermal annealing in the structural and morphological evolution was then correlated with the changes in the optical behavior of the samples. Significant structural and morphological changes were observed, consisting on the crystallization of Ag and their clustering. Clusters growth as a function of temperature was also observed by the evolution of the diffractograms with the temperature increase. The present study allowed to conclude that at certain concentrations (close to 10 at. %), the films revealed some important changes on the optical properties, commonly known as Surface Plasmon Resonance, SPR. This change in the optical behavior of the films was found to be in accordance with the clusters growth as concluded from the evolution of the diffraction patterns. The optical changes, and the correspondent Surface Plasmon Resonance effect were confirmed by reflectivity and CIELab colour measurements. The samples with lower Ag content (11 at. % and 7 at. %) show typical interferometric behavior on the reflectivity curves, similar to those of "pure" TiO_2 samples. After a minimum of reflectance at 300 nm, there was an increase of the reflectivity at higher wavelengths. For the samples annealed between 400 and 600 °C, a red-shift centered at around 500-550 nm is visible in the absorbance spectrum.

(Received January 3, 2011; accepted January 26, 2011)

Keywords: Magnetron sputtering, Surface plasmon resonance, Optical properties, Decorative thin films, Silver, TiO_2

1. Introduction

Noble metal nanoparticles thin films are becoming an intensive area of research due to their interesting functional properties, including the possibility to have extensive colorations [1]. On the other hand, nanocomposite films consisting of noble metal nanoparticles, embedded in dielectric oxide matrixes, are being studied to be used in a wide range of applications, including those of catalysis, photocatalysis, sensors and novel optoelectronic devices [2]. Noble metal nanoparticles such as Ag and Au are known to have free conduction electrons that bring the Surface Plasmon activity [3]. On the other hand, titanium oxide, TiO_2, is one of the most commonly used functionally active matrices because of its chemical stability, high refractive index, and high dielectric constant [2]. In structural terms, TiO_2 is commonly prepared either in amorphous or crystalline types, where the anatase (body-centered tetragonal, BCT) and the rutile (tetragonal, T) are the most typical ones. The TiO_2 (in the anatase form) is a well-known photocatalytic material, with some interesting features such as those of being highly chemically stable and optically transparent [3]. Some investigations indicated that very thin layers of noble metals on TiO_2 surface can capture the photoinduced electrons or holes, eliminating the recombination of electron–hole pairs effectively and also extend the light response of TiO_2 in the visible light region [4]. Furthermore, nanoparticles of noble metals incorporated into a TiO_2 matrix are known to be able to improve its catalytic sensing and optical properties [5].

In terms of decorative-based applications, it is widely accepted that the brilliant colors of noble metal nanoparticles are due to the so-called Surface Plasmon Resonance (SPR) absorption, which is governed by the nanoparticles size, shape and distribution and also by the dielectric constant of the surrounding medium [3]. Therefore the control of size, dispersion, shape and homogeneity of such nanoparticles (nanoclusters) may offer a good possibility to control inventing devices and technologies that have potential uses across several industrial sectors [1]. The present works shows that the change in these key factors can be achieved and monitored by rather simple annealing treatments of the samples.

Regarding the preparation technologies, the TiO_2 with noble metals such as Ag (or Au) nanocomposite materials can be prepared in a number of different ways, where the most frequently used techniques include the chemical photoreduction of Ar ions into porous TiO_2 matrix or on the TiO_2 bulk surface, and the sputter deposition of TiO_2 and Ag [6]. Naoi *et al.* [7] suggested several applications,

including rewritable or electronic paper, for the photochromic TiO_2 films doped with Ag, once they can be easily prepared and applied to large areas. Magnetron sputtering arises as one of the simplest and inexpensive method to achieve these requirements and many other applications [3]. Taking into account the possibility to use such nancomposites in decorative applications, a detailed study of their optical properties will be carried out in this paper and correlated with the structural features.

2. Experimental procedure

Three sets of Ag:TiO_2 thin films were deposited onto silicon (100) and quartz substrates by dc reactive magnetron sputtering, in a laboratory-sized deposition apparatus. For the depositions, a Ti target (99.6 % purity) was used, containing different amounts of incrusted Ag pellets (with 60 mm^2 surface area and approximately 2 mm thickness, and denominated hereafter as Ti-Ag target), symmetrically incrusted in its preferential eroded zone. A constant dc current density of 100 A m^{-2} was applied. A mixture of argon and oxygen was injected with constant fluxes of 60 sccm and 12 sccm, corresponding to partial pressures of 0.3 Pa and 0.08 Pa, respectively. The final working pressure (~0.38 Pa) was kept approximately constant during the entire coating deposition process. Samples were placed in a substrate holder, which was placed in a simple rotation mode (7 rpm). The substrates were biased (- 50V) and the deposition temperature was set to a value of approximately 150 °C (an external heating resistance positioned at 80 mm from the substrate holder was used to heat the samples). A thermocouple was placed close to the surface of the "substrate holder" on plasma side (not in direct contact, since depositions were done in rotation mode), and the temperature was measured immediately after stopping the discharge.

All samples were heat treated through annealing experiments, in vacuum, after film deposition. Annealing treatments were carried out in a secondary vacuum furnace, after its evacuation to about 10^{-4} Pa. The selected temperature range varied from 200 to 600 °C, and the isothermal period was fixed to 60 min, after the required heating ramp of 5 °C/min. The samples cooled down freely in vacuum before their removal to room conditions. Furthermore, chemical uniformity of the films throughout their entire thickness was check by Rutherford backscattering spectrometry (RBS), carried out in a IBA Data Furnace NDF v9.2e at 2 MeV with He^{2+} with an scattering angles of 140° (standard detector) and 180° (annular detector) and incidence angles of 0 and 20° [8,9]. All coatings were characterized by X-ray diffraction (XRD), using a Philips PW 1710 diffractometer (Cu-Kα radiation), operating in a Bragg - Brentano configuration. XRD patterns were deconvoluted, assuming to be Voigt functions to yield the peak position, integrated intensity and integrated width (IntW). These parameters allow calculating the interplanar distance, preferential orientation and grain size. Optical properties (transmittance-absorbance, colours) were characterized using a UV–Vis–NIR Spectrophotometer (Shimadzu UV 3101 PC) in the spectral range from 200 nm to 900 nm. TEM images of the coatings have been obtained by a Jeol 2200 FS transmission microscopy. Color specification was computed under the standard CIE illuminant D65 (specular component excluded) and represented in the CIE 1976 L*a*b* (CIELab) color space [10,11].

3. Results and discussion

3.1. Chemical composition and optical characterization

Table 1 summarizes the fundamental characteristics of the three co-deposited Ag:TiO_2 series of samples. During this work, the films will be denoted as is ascribed in Table 1.

Concerning the chemical composition, RBS analysis revealed that the Ag content ranged from 7 to 20 at. %, showing a roughly linear relationship between the number of Ag pieces in the Ti target and the Ag content in the films. The Ag volume fraction, f_{Ag}, was determined as being in the range between 0.11 and 0.27 (considering $\rho(Ag) = 10.4$ g/cm^3 and $\rho(TiO_2) = 4$ g/cm^3).

The surface coloration of the samples evolved from a green-brownish tone, characteristic of the as-deposited films, to a light purple color tone after the annealing treatment at 300 ºC.

Table 1. General conditions and characteristics of deposited films.

Film series	Ag pellets	Thickness (nm)	Ag (at. %)	*Ag volume fraction, f_{Ag}
A	4	650±50	20	0.29
B	2	650±50	11	0.17
C	1	650±50	7	0.11

*considering $\rho(Ag) = 10.4$ g/cm^3 and $\rho(TiO_2) = 4$ g/cm^3

With the increase of the annealing temperature, the samples were firstly found to reveal some darkening of their surface purple tones, and finally to turn to dark purple for annealing temperatures around 600 ºC. All the Ag:TiO_2 films were reflective. The purple tinge of the samples is more intense for the samples from series B and series C witch present a silver content of 11 at. % and 7 at. %, respectively. For the samples from series A, which presented higher Ag contents (around 20 at. %), the purple color was always paler.

The influence of the Ag clusters size embedded within the dielectric matrix on the SPR activity was accessed, firstly, by reflectivity measurements, shown in Fig. 1. The reflectance spectrum for series A (Fig. 1a.) shows a clear intrinsic behavior at the highest temperatures [12], where after a minimum of reflectance at 300 nm, there is an increasing of the reflectivity at higher wavelengths. The peaks observed around 350 nm for samples annealed above 300 ºC can be attributed to the Plasmon peak of spherical Ag nanoparticles at 400 nm [13].

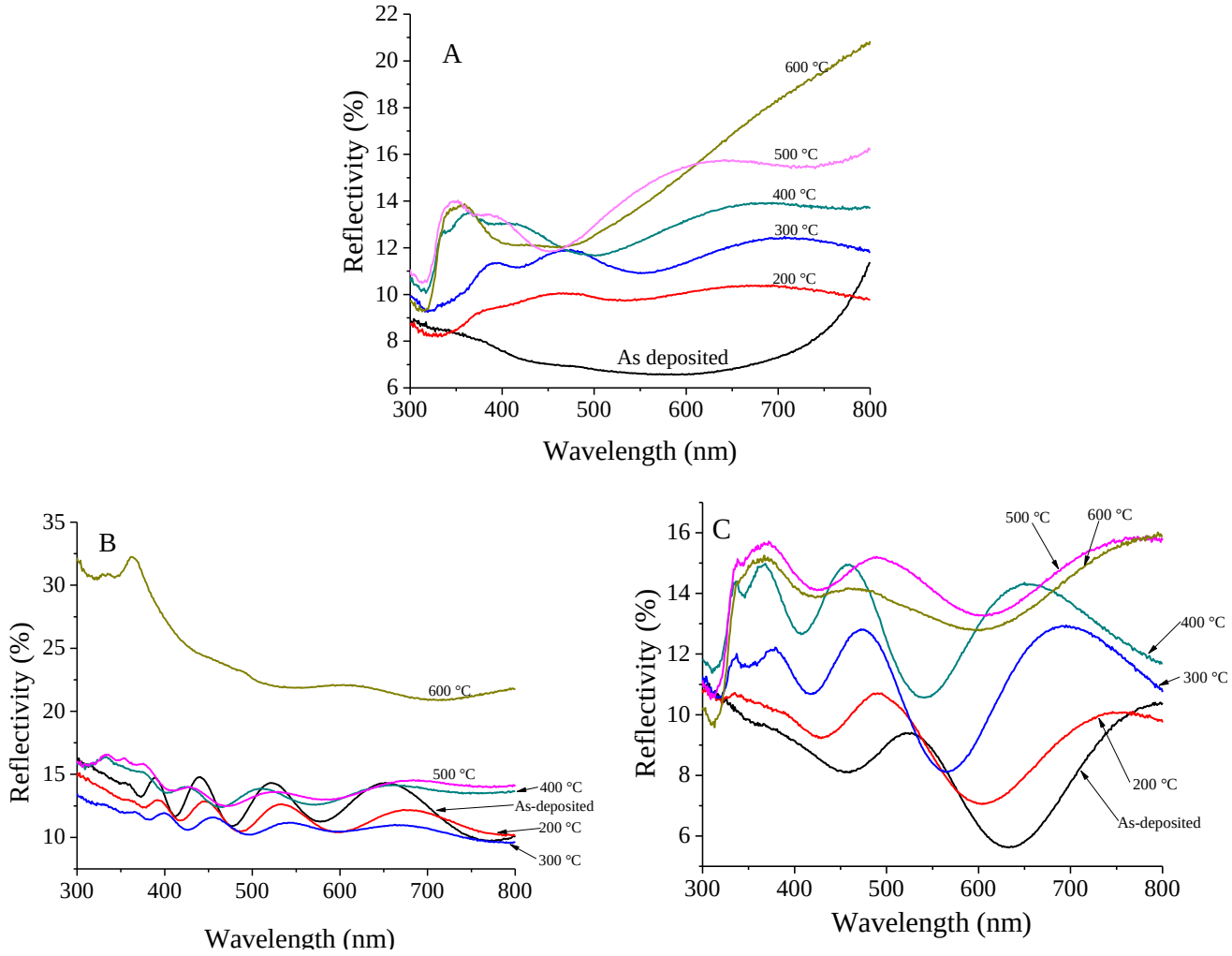

Fig. 1. Variation of reflectivity as a function of annealing temperature (a) for series A, (b) for series B, (c) for series C.

Different reflectivity behavior was found for the samples from series B and C, if one compares the annealed samples with the as-deposited ones. The interference-like behavior disappears after 300 ºC, as it can be observed in Figure 1b and 1c, respectively. The reflectance spectra shows a clear change from interference-like (interference bands are clearly visible for the as-deposited, 200 and 300 ºC annealed samples) to an intrinsic behavior, with the increase of the annealing temperature. The change from one behavior to the other is revealed by the coating's surface tones that tend rapidly to a light purple color, when compared with the as-deposited, 200 ºC and 300 ºC annealed samples. The interference-like behavior is not obvious for the samples from series A, which present higher Ag content. The different spectral dependence of the reflectivity for Ag arises from the position of the d-bands, which cause the difference in color. For Ag, the d-band lies 3.97 eV below the Fermi level, which corresponds to a wavelength close to 300 nm (~313 nm) [14].

In order to better characterize the Surface Plasmon Resonance (SPR) activity, which should be related with the optical changes above described, absorbance measurements (A = log 1/T) were also carried out in the overall sets of samples. Figure 2 shows optical-absorption spectra for varying annealing temperatures for the three series.

The data shown in the Fig. 2 reveals that the as-deposited films have a slight absorption, which is characteristic of Ag particles. This is probably because of the fine dispersion of such particles. The same behavior can be observed for the samples annealed at 200 and 300

°C. The absorption edge below 400 nm is due to the interband transition in the TiO_2, which has a band-gap energy of about 3.2 eV [3]. For the samples annealed at 400 °C, a red-shift centered at around 500 nm is visible, while for the samples annealed at 500 and 600 °C there is a red-shift of the peak until 550 nm. This is caused by the particle-Plasmon Resonance of the Ag nanoparticles.

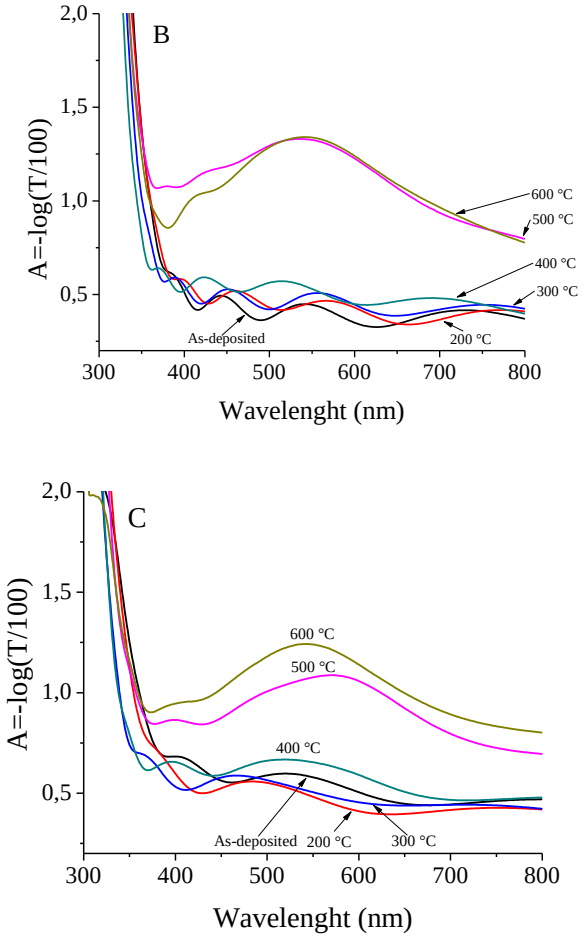

Fig. 2. Absorbtion spectra as a function of annealing temperature for (a) series A, (b) series B, (c) series C.

This resonance is inhomogeneously broadened, which is most probably due to a broad distribution of particle sizes and shapes in the films, and due to the possible inhomogeneities in the dielectric environment of the particles [2], as we have in fact demenostrated to a similar system composed of Au [9]. The maximum of the absorbance spectrum is shifted to higher wavelengths upon annealing at 500 °C. An increase on the nanoparticle size generally leads to a red-shift of the resonance position [3], again in accordance to what was observed for Au [9]. The red shift of Ag:TiO_2 can be ascribed also by the variance in the dielectric constant of titanium oxide matrix that probably exists as a consequence of different ratios of amorphous/anatase phases, arising from the different annealing treatments [9]. The matrix presents a different dielectric constant for each annealing temperature modifying the energy of the SPR absorption, located at larger wavelengths for more crystalline matrixes (higher annealing temperatures). The amount of silver initially present in the system determines the maximum particle size attainable and therefore controls the long-wavelength absorption of the system [15]. Similarly, the annealing temperature controls the aggregation processes responsible for the growth of the silver nanoparticles [15]. Both parameters together allow the tuning of the absorption properties in the visible range [3]. The differences in the intensity observed on the reflectivity curves are in good agreement with the absorbance curves. Globally, at the same wavelength, higher reflectivity is linked to lower absorbance intensity. The maximum of the absorbance spectrum is achieved upon annealing at 600 °C. As one can observe from Fig. 2, the absorbance picks with better defined shape are ascribed for the films from series B and series A that present relatively low silver contents. One can observe that the absorption peak become broader as the volume fraction of silver nanocrystallites increases to 0.29 (Fig. 2a). This behavior can be explained by the increase in size distribution that led to the broadening of the surface Plasmon absorption peak [13].

3.2. Morphological and structural characterization

In order to scan the changes that ere induced in the films by the annealing process, and thus to understand their effects in the observed changes in the samples optical behavior, a detailed analysis of the morphology and structure was carried out by both TEM and XRD. The morphology of the as-deposited films was found to be quite similar for the three different series (Fig. 3a), consisting of Ag agglomerates dispersed in the TiO_2 matrix, changing in shape, size, distribution and crystallinity as a function of the different annealing temperatures (Fig. 3b). As an example, Fig. 3 shows TEM micrographs obtained from samples from series B. From the cross-sectional view, one can observe that the Ag particles have a broad size and shape distribution; with lateral diameters varying from a few nanometers to about 50 nm, as estimated from the TEM micrographs. Important to note is that the larger clusters are located at the interfaces, especially on that with the substrate.

Anyway, the TEM preparation procedures do not allow having an accurate view of the outer surface (due to the sample preparation procedures), and thus it is not easy to claim any conclusion about this other interface. The same behavior has been also claimed by *Sella et al.* [16], which found that the Ag nanoparticles are in the immediate vicinity of the Si substrate. In agreement with TEM results, the broad absorption that the samples presented (as dicussed in the previous chapter, Fig. 2) can be related, as in fact expected, also to the presence of more closely interacting metal particles.

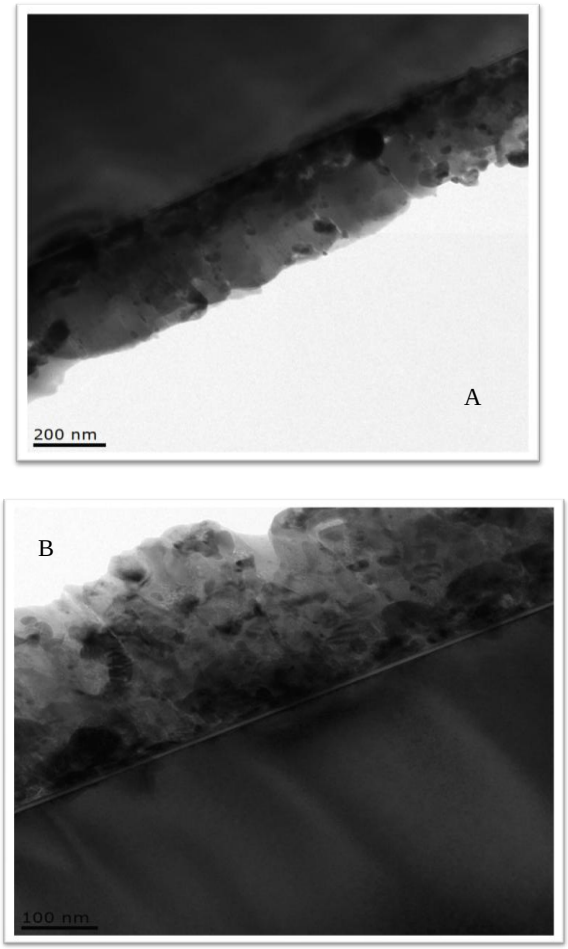

Fig. 3. Cross-section TEM micrographs for as deposited sample from serie B. a – as-deposited sample; b – 500 °C annealed sample.

In order to follow the influence of the developed crystallinity in the different samples, as well as the particular evolutions in the grain sizes (which were not easily characterized in the TEM analysis) in the films, a detailed structural characterization was carried out in all prepared films. The XRD patterns of the nanocomposite films (Fig. 4) illustrate the crystalline state of the Ag in the samples from series A, for all analyzed samples. Important to note is that all three series presented similar trends and thus only series A will be shown in detail.

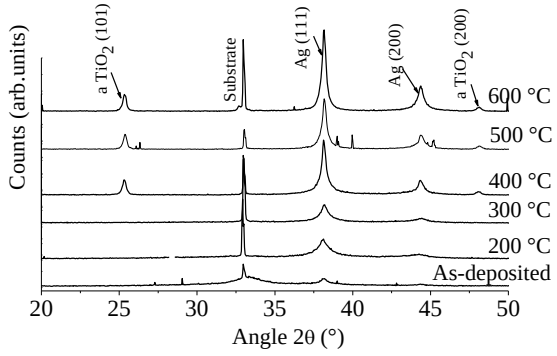

Fig. 4. XRD patterns for the different annealed samples from series A.

All the Ag films are crystalline, showing an fcc-Ag structure [ICDD card N° 04-0783], as it can be observed by the presence of (111) peak, localized at 2Θ = 38.11°. An increase in temperature of the thermal treatment (above 300 °C) resulted in an intensity increase of this peak, along with the appearance of a second signal at 2Θ = 44.27°, ascribed to the (200) Ag planes. The first important note that is worth being mentioned is that by allowing diffusion and coalescence phenomena, the thermal annealing lead to a progressive growing of the Ag clusters. In fact, the enhancement of the intensity and the narrowing of the XRD peaks assigned to the fcc-Ag structure as the annealing temperature increases are evident, which is a clear sign of increasing crystallinity. As mentioned before, and except for the variation in the intensity of the picks, the three sets of samples present the same structural behavior.

The first XRD profile show the scan performed on the as-deposited sample, where the only clear feature is the diffraction peak obtained at 2Θ around 38.1°. The intensity of this diffraction peak is very low, which indicates that Ag is most probably finely dispersed in the amorphous TiO_2 matrix. In contrast to as-deposited samples, XRD results of films annealed at temperatures between 400 and 600°C show pronounced Ag peaks. In accordance, one can claim that the Ag particles have been formed and grown inside the TiO_2 dielectric matrix.

Other additional peaks are present for the annealing at higher temperatures (as compared with the samples annealed at 200 and 300 °C). Anyway, it is important to note that sputter deposited "pure" amorphous TiO_2, are commonly reported to crystallize in the form of anatase after annealing at a temperature around 300 °C [3]. In contrast, the crystallization of TiO_2 doped with Ag is delayed, as observed in this works' results, Fig. 4. According to the XRD patterns, the film remains amorphous after annealing treatment at 300 °C. During the annealing at 400 °C, the amorphous TiO_2 matrix crystallizes in the anatase form [ICDD 21-1272] as in fact suggested in similar studies where annealing of TiO_2-based films is involved [9]. The access of this nanocomposite structure up to 300 ºC could be responsible for the appearance of SPR activity that can be used to tune some of the film properties, namely the optical ones, as it has been showed in this text. The delayed crystallization is another indication of the fine dispersion of Ag in the amorphous TiO_2 matrix during the sputter process. The presence of Ag atoms appears to increase the activation barrier for crystallization [3]. Similar phenomena have also been reported for an incorporation of Fe in TiO_2 [17] and for sol-gel-prepared Ag:TiO_2 films [18].

Important also to emphasizes is that similarly to the morphological features, there is also a straight correlation between the interference-like and intrinsic-like behaviors of the samples and the XRD results. In fact, this behavior in the reflectance spectra occurs because of the presence of Ag nanoparticles. Ag clusters coalescence, seems to confirm the major role of morphological and structural changes in the films behavior. The relatively low values of

the reflectivity at shorter wavelengths are characteristic of high free electron density systems [19].

As an example of common behaviour Fig. 5 presents the evolution of average size (diameter) of the silver particles in the nanocomposite films for the samples from series B, as a result of the peak fitting procedure. The results are based on the integral-breadth of the XRD patterns. The Ag particles sizes are increasing with the increase of annealing temperatures. No significant Ag crystallite size variation is observed during annealing from 300 to 600 °C. The values of silver particles (clusters) size range from about 12 nm at 300 °C to 17 nm at 600 °C. The related changes on the optical properties and the SPR activity can also result from the growth of Ag nanoparticles. The main SPR activity has been reported between 400 and 600°C, where the average grain size is within 15 nm. SPR effect might be also present on the first annealed samples, but they are clearly more evident for the highest temperatures. At low annealing temperatures the SPR is low, due to interaction among the nanoparticles. Higher annealing temperatures lead to higher grain size and increase the distances between the Ag clusters, as in fact confirmed by the TEM observations. At 600 ºC they reach the optimal distance and the SPR effects are more intense. At 400 ºC, the XRD peaks becomes narrower because there is a predominant grain size, larger and more crystalline, which is more sensitive to the particles interaction, giving the main SPR. The absorbance edge shifts towards lower wavelength with increasing temperature. This rise is attributed to the crystallization process and the resultant increase in the grain size by the annealing. The increase of grain size is linked with the main changes on the reflectivity and color analysis. Better crystallinity of the films i.e larger grain increases the optical reflectance.

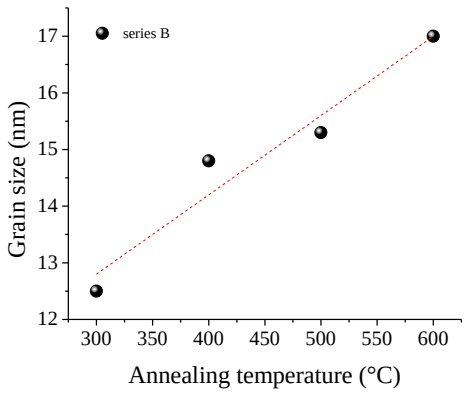

Fig. 5. Variation of grain size as a function of annealing temperature of series B.

4. Conclusions

The presented “one step” co-sputtering method was used to prepare Ag:TiO_2 films. The deposited films were subjected to annealing treatment at different temperatures. It is demonstrated that the SPR activity of the Ag nanoparticles can be monitored.

Structural conditions to reach SPR are achieved for samples annealed above 300 °C. The structural conditions are influenced by two different parameters, (i) amount of Ag silver doping the dielectric TiO_2 matrix and (ii) grain size of the Ag nanoclusters that can be controlled by the annealing temperatures of the samples after the deposition. The growth of silver nanoparticles and their redistribution in the dielectric matrix are the main factors for the presence of SPR. The TiO_2 phase or crystalline matrix ratio seems to play a secondary role, shifting the position of the SPR bands at higher wavelengths. The evolution of the reflectivity is in accordance with the XRD results and with the changes on crystal grain size. In the as-deposited films, a small silver pick is evident, which indicates that the silver is finelly dispersed in the amorphous matrix. Upon annealing, silver nanoparticles are formed and peaks (Ag) can be observed in the XRD profiles. Annealing at 400 °C results in the crystallization of the TiO_2 into the anatase phase (A). The grain size of the Ag nanoparticles show a rapid growth with annealing treatment at different temperatures. The annealed films from all the three series show a broad absorption band across the visible range caused by the particle-plasmon resonance of the Ag nanoparticles. Increasing the annealing temperature leads to the formation of larger particles absorbing at longer wavelengths. It can be conclude that sputtered Ag:TiO_2 thin films can be appropriate for decorative applications due to their optical properties.

Acknowledgments

This research is sponsored by FEDER funds through the program COMPETE - Programa Operacional Factores de Competitividade and by national funds through FCT - Fundação para a Ciência e a Tecnologia, under the project PTDC/CTM/ 70037/2006.

References

[1] G. Walters, I. P. Parkin, J. Mater. Chem. **19**, 574 (2009).
[2] M. G. Manera, J. Spadavecchia, D. Busoc, C. de Julian Fernandez, G. Mattei, A. Martucci, Mulvaney, J. Perez-Juste, R. Rella, L. Vasanelli, P. Mazzoldi, Sens. Act. B **132**, 107 (2008).
[3] J. Okumu, C. Dahmen, A. N. Sprafke, M. Luysberg, G. von Plessen, M. Wuttig, Appl. Phys. **97**, 094305-1 (2005).
[4] H. Y. Chuang, D. H. Chen, Nanotechnology **20**, 105704 (2009).
[5] G. C. Bond, Catal. Today **72**, 5 (2002).
[6] J. Preclíková, P. Galár, K. Žídek, F. Trojánek, P. Malý, J. Nanosci. Nanotechnol., **10**, 2630 (2009).
[7] K. Naoi, Y. Ohko, T. Tatsuma, J. Am. Chem. Soc. **126** (11), 3664 (2004).
[8] N. P. Barradas, C. Jeynes, R. P. Webb, Appl. Phys. Lett. **71**, 291 (1997).
[9] M. Torrell, L. Cunha, A. Cavaleiro, E. Alves, N. P.

Barradas, F. Vaz, Appl. Surf. Sci. **256**, 6536 (2010).
[10] Colorimetry, CIE Publ. (Commission Internationale de L'Éclairage) 15 (1971).
[11] Recommendations on Uniform Color Spaces, Difference-difference equations, psychometric color terms, CIE Publication, No 2-70 (Commission Internationale de L'Éclairage) 15 (1978).
[12] A. R. Malagutti, A. J. L. Mourao, J. R. Garbin, C. Ribeiro, Appl. Catal. B-Environmental **90**, 205 (2009).
[13] J. Yu, J. Xiong, B. Cheng, S. Liu, Appl. Catal. B **60**, 211 (2005).
[14] H. Ehrenreich, H. R. Philipp, Phys. Rev. **128**, 1622 (1962).
[15] M. Torrell, P. Machado, L. Cunha, N. M. Figueiredo, J. C. Oliveira, C. Louro, F. Vaz, Surf. Coat. Technol. **204**, 1569 (2010).
[16] C. Sella, S. Chenot, V. Reillon, S. Berthier, Thin Solid Films **517**, 5848 (2009).
[17] W. Zhang, Y. Li, S. Zhu, F. Wang, Chem. Phys. Lett. **373**, 333 (2003).
[18] E. Traversa, M. L. di Vona, P. Nunziante, S. Licoccia, J. W. Yoon, T. Sasaki, N. Koshizaki, J. Sol-Gel Sci. Technol. **22**, 115 (2001).
[19] L. Yate, L. Martínez-de-Olcoz, J. Esteve, A. Lousa, Vacuum. **83** (10), 1287 (2009).

*Corresponding author: mtorrellfaro@gmail.com